A STUDY OF SWITCHING OVERVOLTAGES IN OFFSHORE WIND FARM

A. H. Soloot[1*], H. K. Høidalen[1] and B. Gustavsen[2]
[1]Department of Electrical Power Engineering, Norwegian University of Science and Technology (NTNU),Trondheim N-7491, Norway.
[2]SINTEF Energy Research, Trondheim N-7465, Norway
*Email: amir.h.soloot@elkraft.ntnu.no

Abstract: Switching transient as one of the main transient phenomena in power systems have been simulated and measured in many studies. Since offshore wind farms have been integrated to power system only in recent years, the consequences of switching phenomena in offshore wind farms have not yet been thoroughly analyzed. This paper contributes to the topic by a study on overvoltages using a high-frequency model of the wind turbine transformers (WTTs).
The WTTs are represented by a black-box high-frequency model obtained from measurements and represented by an equivalent RLC network for inclusion in ATP-EMTP. The model represents a 300 kVA 11.0/0.230 kV transformer.
The resonance frequencies observed at the Low Voltage (LV) and High Voltage (HV) terminals of the transformer are found by voltage ratio and impedance matrix simulations using the derived high frequency transformer model. The simulation results indicate that the dominant resonance frequency of this transformer in terms of voltage ratio from the HV side to the LV side appears at 2 MHz.
In energization of a wind turbine, the critical cable length leading to transformer resonance overvoltages and the impact of surge arresters on LV and HV are investigated. The simulation results indicate that the LV surge arrester have prominent role in limiting the resonance overvoltages although the ground lead inductances some how decrease the effect of surge arresters.

1 INTRODUCTION

The number of Offshore Wind Farm (OWF) installations in Europe has grown significantly in the last decade. Although the first OWF was installed in Vindeby, Denmark in 1991, the development of OWF was not significant during 1990-2000. However the share of OWF in wind power market has later been drastically increased from 0.12% to 9.5% during 2000-2010 [1]. By installing OWFs at more distance from the shore, more power can be harnessed from the OWFs.

Due to the increased distance of OWFs from shore and adverse weather conditions in oceans, a main criterion in OWF design and operation is high reliability, with little maintenance. Therefore, many studies have focused on potential technical hazards in OWF, especially overvoltages due to switching transients [2]-[5].

Switching transients consist of both energization overvoltages and disconnection ones. Besides, earth faults can be viewed as a switching to earth.
Since OWF consists of a series of cable-transformer connections, the energization of OWFs can lead to resonance overvoltages when the travelling wave frequency of energized cable equals to dominant resonance frequency of Wind Turbine Transformer (WTT). In [6], the general criterion for resonance overvoltages in cable-transformer connection is studied and various connections are surveyed.

First aim of this paper is to simulate and analyze the energization overvoltages in OWFs. The second aim is to discuss the conditions which can lead to resonance overvoltages. The role of surge arrester in diminishing the amplitude of resonance overvoltages is also investigated.

2 OFFSHORE WIND FARM MODELLING

Modelling of OWFs depends on the aim of analysis. In [7], it is shown that for analyzing the 3-phase to ground fault in grid connected to OWF, the aggregated model of OWF can give good results for Point of Common Coupling (PCC) voltage, active and reactive power. Whilst the aggregated model which consider the whole OWF as a generator with a power equal to the sum of wind turbines power is not sufficient to model the transient overvoltages in disconnection of OWF from grid [4]. Since the overvoltages inside OWF rows is investigated in this paper, the detailed model of OWFs with consisting components should be considered.

The main components in OWFs for the switching transient investigations are WTTs, cables and

Vacuum Circuit Breakers (VCB). In this paper, the OWF row considered for simulation is illustrated in figure 1. It consists of five WTTs which are connected in a row with five cables for interconnection. There are five VCBs to switch the WTTs and one VCB for switching the row. This row is simulated and analyzed in Alternative Transient Program (ATP).

VCBs have multiple prestrike and multiple reignitions in energization and de-energization, respectively which can mainly effect the amplitude and waveform of overvoltages in OWF [2]. Since the focus of this paper is on resonance overvoltages in OWF, the VCB can be simply modelled as ideal switch. For representing the WTTs in ATP, we used a wide-band model of a 300 kVA 11/0.230 kV transformer developed in [6]. This model was obtained by terminal frequency sweep measurements and black box model extraction. Here, the following steps were taken.

1. The 6×6 admittance matrix of 11.4kV/0.230 kV, 300 kVA transformer was established by measurements as functions of frequency from 10 Hz to 10 MHz. The coaxial measurement cables were compensated for.
2. The black box model of the transformer was obtained based on vector fitting [8]-[9] followed by passivity enforcement by residue perturbation.
3. An equivalent RLC lumped parameter network was generated from the rational model and implemented in ATP-EMTP via “User Specified Library” elements.

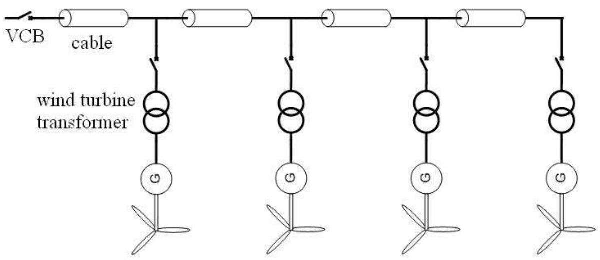

Figure 1: Offshore wind farm system

For cable modeling, the JMarti model is used. The JMarti model considers the transformation matrix as a frequency independent matrix and computes it for a fixed, single frequency, which is chosen in the vicinity of the dominant frequency components in the simulation. These frequencies are established according to the cable resonant frequencies which are related to the cable length. The cable geometry data are shown in table 1.

The characteristics of surge arrester applied in LV and HV terminals of transformer are based on ABB POLIM-R-2N [10] and POLIM-C..N [11] and are shown in table 2 and 3. In the datasheet of the surge arresters, V-I characteristic for segment I>1 kA is given. For I<1 kA , V-I data is considered in a way that the log-log plot of V-I characteristic become as linear as possible. It is due to the mathematic modelling of different segments of surge arrester to fit the following equation,

$$i = p\left(\frac{v}{V_{ref}}\right)^{q} \tag{1}$$

where p is the exponent, q is the multiplier for that segment, and V_{ref} is an arbitrary reference voltage that normalizes the equation and prevents numerical overflow during exponentiation. It should be mentioned that an inductance of 1 µH per meter should be considered for ground lead of surge arrester. Because inductances play role in high frequency.

Table 1: Cable geometrical parameter

Parameter	Value
core inner radius (m)	0
core outer radius (m)	0.02
core resistivity (ohm×m)	1.72×10^{-8}
core permeability (H/m)	1
core-sheath insulation permittivity (F/m)	2.671
sheath inner radius (m)	0.035
sheath outer radius (m)	0.038
sheath resistivity (ohm×m)	2.2×10^{-7}
sheath insulation permittivity (F/m)	2.3
Surge velocity in XLPE cable (m/s)	1.85×10^{8}

Table 2: LV surge arrester parameters (ABB Polim-R-2N)

Peak current (A peak)	Residual Voltage (V peak)
0.0001	154
0.001	160
0.01	180
0.1	210
1	235
10	245
100	270
1000	290
1500	300
3000	310
5000	320
10000	330
20000	340
40000	380

For Modelling LV side of transformers, depending on the wind turbine configuration [13], soft start or full-scale frequency converters can be on LV side of transformers. In the energization of WTT, the soft-start or frequency converter is started after the energization of transformer. Therefore, they are off and depending on the manufacturers, the output capacitance of IGBTs in frequency converter can be in range of 0.5-1.5 nF. Besides, capacitor banks for asynchronous generators can be in the range of some hundred microfarads up to some millifarads. To sum up, they should be included based on the wind turbine under study.

Table 3: HV surge arrester parameters (ABB Polim-C..N)

Peak current (A peak)	Residual Voltage (V peak)
0.0001	9240
0.001	11000
0.01	12500
0.1	13800
1	14500
10	16000
100	17000
1000	19300
2500	20600
5000	21500
10000	22700
20000	25200

3 SIMULATION RESULTS

As explained in the previous section, the high frequency black box model of the WTT, which is achieved from measurement, is applied. In this way, a better understanding of overvoltage induction on the both High Voltage (HV) and Low Voltage (LV) side can be obtained. The latter can be quit critical for wind turbine low voltage equipment such as power converter and generator.

The frequency spectrum of impedance and voltage ratio matrices of WTT was investigated in previous work [14]. Besides, the resonance frequencies and the dominant one were determined by these frequency spectrums. It should be mentioned that, resonance overvoltages can happen in OWF due to harmonic injection of power converters [15]. But, the harmonic resonances frequencies are lower that 1kHz.

In this paper, a review on frequency spectrum of WTT terminals is discussed in 3.1. The effect of load capacitances in LV side of wind turbines is studied in 3.2. The role of surge arresters on WTT protection is investigated in 3.3. Finally, the energization transient of second wind turbine row while the first one is already connected is analyzed in 3.4.

3.1 Cable-Transformer Energization

In order to have better observation on the effects of a detailed high frequency transformer model on terminal voltage and currents, a no-load transformer is energized with a cable-transformer configuration as shown in figure 2. The energization is at the moment of positive maximum value for phase A, which is the most critical switching. Since the FFT is applied on one period of 50 Hz, the initial frequency in the spectrum is 50 Hz.

The frequency spectrum of HV and LV voltages are illustrated in Figure 3 as well as HV current. It can be observed that the frequency spectrum of HV current is in agreement with LV voltage rather than HV one in frequencies lower than 10 kHz.

The resonance frequencies (frequency peaks) can be observed in figure 3. The first peak after 50 Hz in frequency spectrums relates to the travelling wave in cable which is inversely proportional to cable length according to (2). The cable length is assumed 500 m in simulation in figure 2 which is a typical wind turbine distance in offshore wind farm.

$$f = \frac{V_{cable}}{4l} \qquad (2)$$

V_{cable} is velocity of surge in XLPE cable which is 1.86×10^{8} m/s according to table 1. Therefore, the travelling wave frequency is 92.5 kHz and JMarti model of cable is around this frequency. A more detailed observation of higher frequency peaks (Figure 4) shows that LV terminal frequency peak not only is comparable with HV one but also exceeds it around 2 MHz. Therefore, 2MHz is a critical resonance frequency and resonance overvoltages occurs in LV terminal if the cable length is such that travelling wave frequency matches with dominant resonance frequency [14].

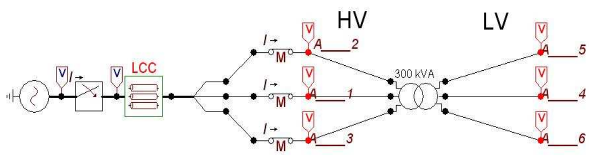

Figure 2: Cable-transformer 3 phase energization circuit on peak voltage. LCC is the cable model in ATP.

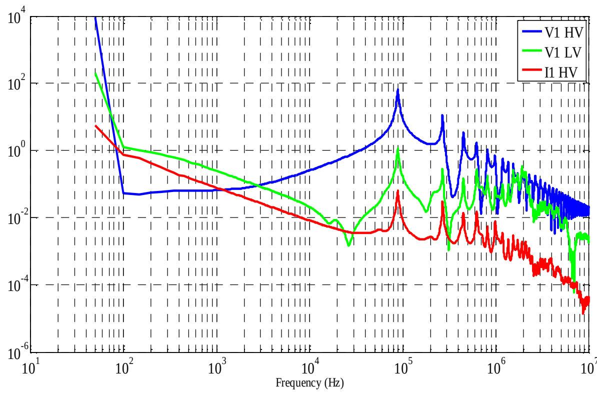

Figure 3: The primary and secondary voltage spectrum of 300KVA 11/0.230 kV transformer which is 3 phase energized via 500 m cable-phase A HV voltage (blue curve), LV voltage (green curve) as well as HV current (red curve).

The frequency spectrum of all transformer terminals is shown in Figure 5 around 2MHz (2MHz=$10^{6.3}$Hz). Since phase A is in the middle limb in the transformer and phase B and C have same amplitude (half negative peak) at the moment of energization, the spectrum of phase B and C is similar in figure 5.

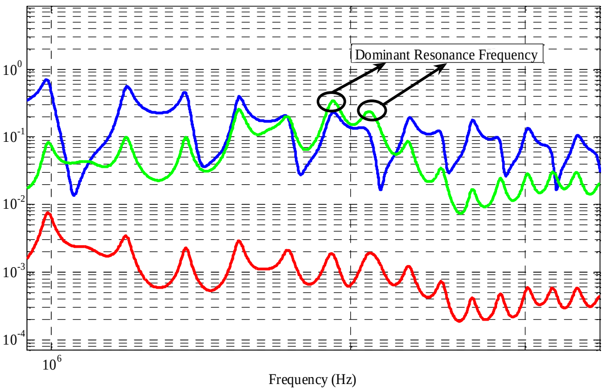

Figure 4: LV terminal frequency peak exceeds HV terminal frequency peak (resonance phenomena).

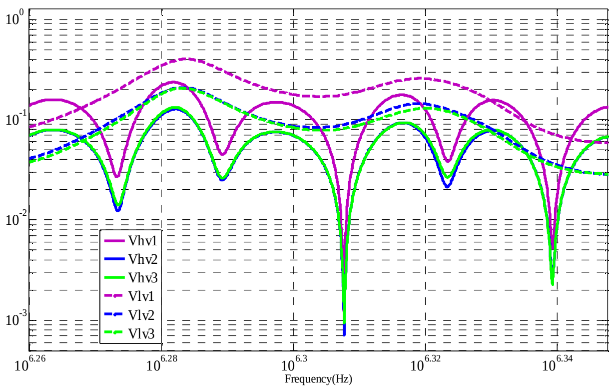

Figure 5: The primary and secondary voltage spectrum of 300KVA 11/0.230 kV transformer. Solid Lines are HV terminal voltages and dotted lines are LV terminals.

It should be mentioned that in designing an offshore wind farm, the frequency analysis of WTT as well as platform transformer should be recognized. The reason is that any switching in OWF, especially WTT energization with cable inside wind turbine tower has the potential to result in resonance overvoltages. Thus, in the following subsections, energization of 300kVA WTT in a wind turbine via 23 meter cable is investigated. According to (2), for having travelling frequency equal to 2 MHz, the cable length should 23 meter.

3.2 Wind turbine load capacitances

In section 2, we discussed about considering the parasitic (stray) capacitance of frequency converter or soft start. As mentioned in previous subsection, the energization of one wind turbine with cable in range of some ten meter (height of wind turbine) is the case with most resonance overvoltage. Therefore the simulation circuit is the same as figure 2. But, the cable length is 23m In this subsection, the effect of equivalent capacitance observed from LV transformer terminal, load capacitance, is examined. The simulation results are shown in figure 6 and table 4.

The base voltage is the LV phase peak voltage in figure 6 and table 4. The load capacitance can either be parasitic capacitance of frequency converter in synchronous generator wind turbine or capacitor bank in asynchronous one. Therefore, a wide range of capacitance is surveyed.

According to table 4 and figure 6, capacitance up to 10 nF diminish significantly the resonance overvoltage amplitude. Besides, the resonance overvoltage waveform is much distorted. Whilst for higher capacitance due to capacitor bank application, the amplitude is not effected so much but the time to first peak (rise time) is increased resulting in smoothing the overvoltages.

It can be concluded that applying capacitors in LV side of transformer can be a remedy for resonance overvoltages. Though, the reactive power regulation should also be considered for steady state operation. Therefore, a compromise for the capacitance value should be done. The capacitance should neither be so small that have no effect nor so large that irritates the functionality of power converter.

It should be mentioned that for a 300 kVA asynchronous wind turbine with 20% reactive power compensation, the value of capacitor bank will be 3.5 mF. Therefore, the resonance overvoltage will be damped if capacitor bank is connected (figure 7). The base value for current is LV peak line current which is 1.065 kA for the 300 kVA transformer. Therefore, capacitor bank inrush current is 1.5 pu. It can be observed that the overvoltage is also damped in 5ms and the phase voltage will be rated voltage later.

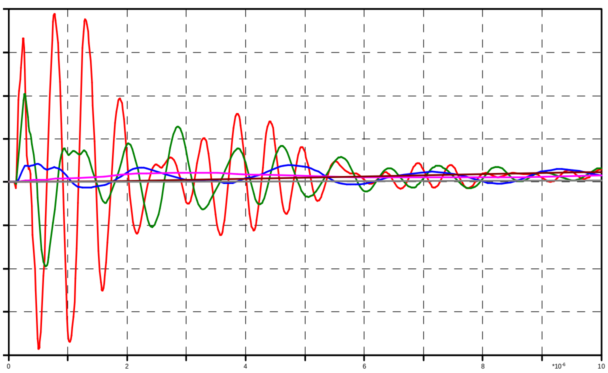

Figure 6: The effect of load capacitances on the LV terminal overvoltages; load capacitances equal to: 0.1 nF for red curve, 1 nF for green curve, 10 nF for blue curve, 100 nF for pink curve, 1 µF for brown curve and 10 µF for gray curve. (time division=1µs, voltage division=7 p.u.)

Table 4: Effect of load capacitance in wind turbine

Load capacitance (nF)	First peak voltage (V)	First peak voltage (p.u.)	Time to first peak (µs)
0.1	4500	24	0.24
1	2750	14.64	0.27
10	500	2.66	0.28
100	270	1.44	2.21
1000	333	1.77	12.13
10000	333	1.77	40.00

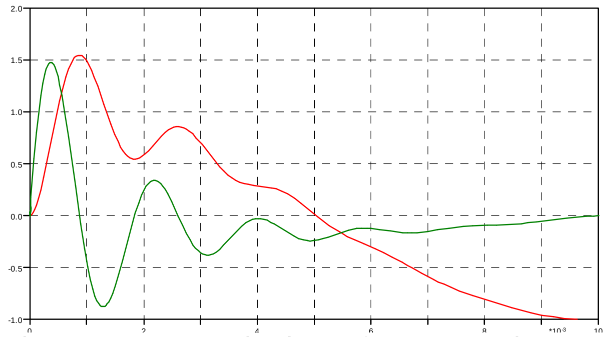

Figure 7: Energization of an asynchronous generator with connected capacitor bank in resonance condition; voltage without surge arrester (green curve), with surge arrester (red curve), arrester current (blue), capacitor bank current (pink). (time division=1ms, voltage and current division=o.5 p.u.)

3.3 Surge arrester in wind farm

Generally, surge arresters are installed on WTT terminals in order to protect them from lightning surges which hit the wind turbine blades or nacelle [16]. In [17], the absorbed energy of surge arrester during earth fault in OWF is also investigated and grounding transformer or fast grounding switch are suggested for diminishing overvoltages in OWF and protecting surge arrester from blowups.

The complete simulation circuit for investigating the effect of surge arrester on resonance overvoltage is shown in figure 8 where the energized transformer is protected with surge arrester on both HV and LV terminals. Since the impact of surge arrester on resonance overvoltage is going to be studied, the cable length is 23 meter as also explained in 3.2.

The importance of including the inductances of ground lead in HV surge arrester (0.5 µH) and LV surge arrester (0.25 µH) is depicted in figure 9. This stray inductances decrease the influence of surge arrester on resonance overvoltages.

In figures 10-13, a full study of transformer terminal voltages in various surge arrester connections are shown. The waveforms of the LV terminal voltages without surge arresters are depicted in figure 10 and 11 for phase A and C in red curve, respectively. Besides, the limited LV terminal voltages due to surge arrester application are compared with LV terminal voltages without surge arrester. As it can be observed in these figures, LV terminal voltages are limited to 2.5 pu. It would be less if there were no ground lead inductances in surge arrester. Thus, it can be observed how important the inclusion of lead inductances is.

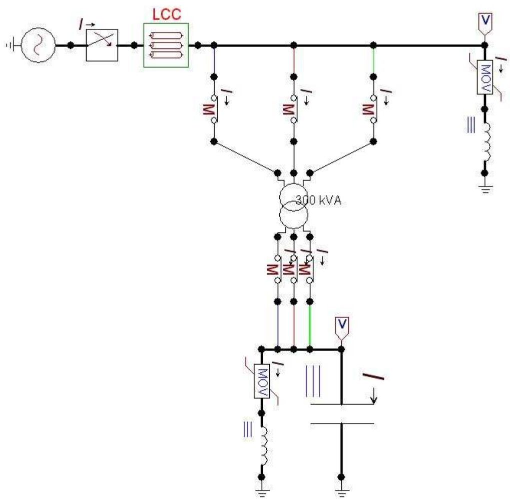

Figure 8: Surge arresters on the LV and HV side of transformer to limit resonance overvoltage.

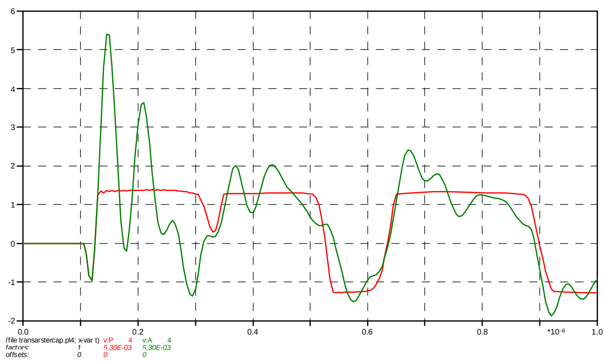

Figure 9: Surge arresters model with inductance for ground leads (green curve), without inductances (red curve). (time division=0.1µs, voltage division=2 p.u.)

As shown in figure 5, the resonance phenomena on LV side in phase B and C are similar since phase A is in middle. Therefore, in addition to HV phase A current, just the LV current waveform of phase A and C are shown in figure 14. Since the transient voltage in phase B and C HV side is lower than 1 pu, their surge arrester does not drain current and perform. The working point of the surge arrester is on the first segment and the maximum current point is approximately 40 A.

It can be concluded that the installation of Surge Arrester (SA) just on HV side, only guarantees the HV terminal from overvoltages and LV terminals have still risk of damage due to resonance overvoltages.

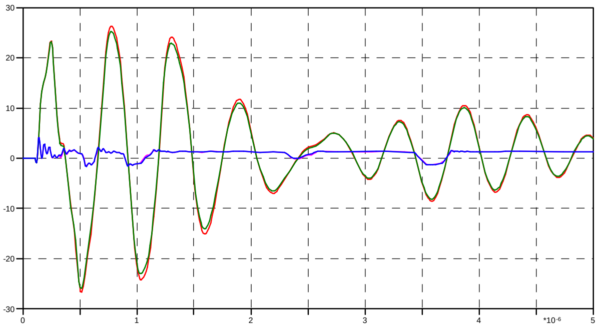

Figure 10: LV voltage on phase A in resonance condition; without surge arrester (red curve), with surge arrester just on HV terminal (green curve), with surge arrester just on LV terminal (blue curve), with surge arrester on both LV & HV terminal (pink curve).(time division=1µs, voltage division=10 p.u.)

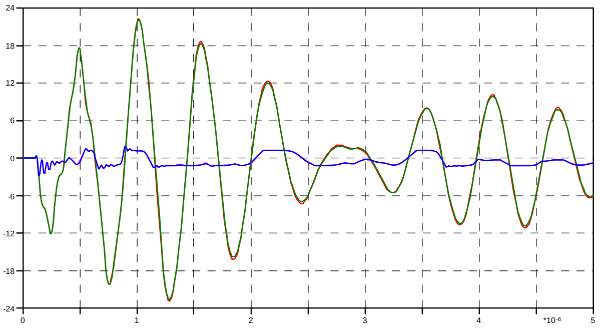

Figure 11: LV voltage on phase C in resonance condition; without surge arrester (red curve), with surge arrester just on HV terminal (green curve), with surge arrester just on LV terminal (blue curve), with surge arrester on both LV and HV terminal (pink curve).(time division=1µs, voltage division=6 p.u.)

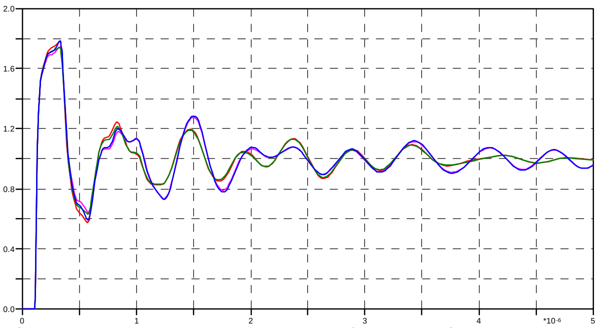

Figure 12: HV voltage on phase A in resonance condition; without surge arrester (red curve), with surge arrester just on HV terminal (green curve), with surge arrester just on LV terminal (blue curve), with surge arrester on both LV & HV terminal (pink curve).(time division=1µs, voltage division=0.2 p.u.).

3.4 Energization of second row

In this section, the energization of a second row is investigated while the first one is already connected (figure 15). Each row represents the configuration in figure 1. The transient voltages at the end of two lines and row connection point are illustrated in figure 16.

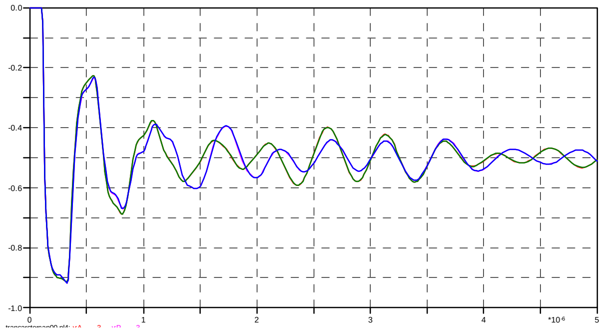

Figure 13: HV terminal voltage on phase C in resonance condition; without surge arrester (red curve), with surge arrester just on HV terminal (green curve), with surge arrester just on LV terminal (blue curve), with surge arrester on both LV and HV terminal (pink curve). (time division=1µs, voltage division=0.1 p.u.).

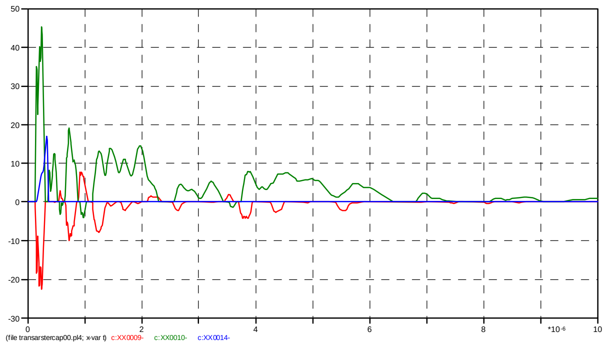

Figure 14: Arrester currents in resonance condition; HV phase A (blue curve), LV phase A (green curve), LV phase C (red curve).

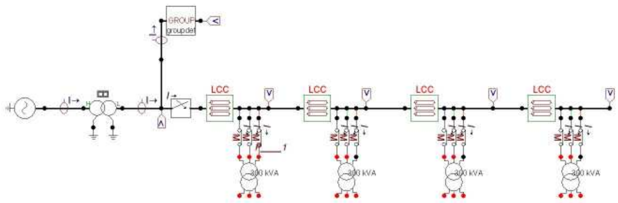

Figure 15: Energization of send wind turbine row in ATP

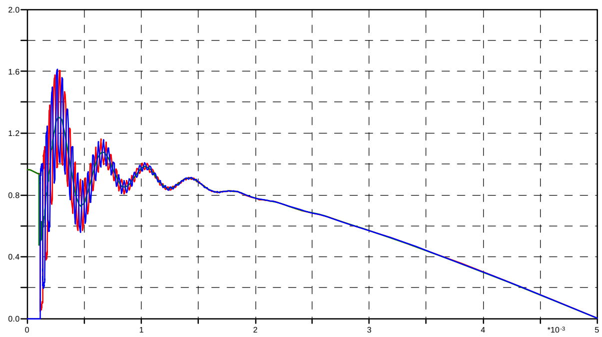

Figure 16: Energization of the second row on maximum voltage; voltage at connection point (green curve), end of first line (red curve), end of energized line (blue curve). (time division=1ms, voltage division=0.2 p.u.).

A closer view in figure 17 shows that the switched row has inverse transient comparing to first row. This can be explained in this way that cable capacitances of the first row which have maximum voltage want to balance with the newly connected capacitances in second row and have same potential. Therefore, the surge which travels in second row has half maximum voltage and a negative surge with half maximum voltage travels in the first line.

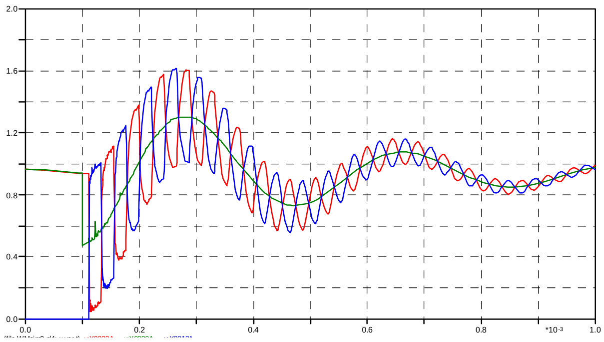

Figure 17: Energization of the second row on maximum voltage; voltage at connection point (green curve), end of first line (red curve), end of energized line (blue curve). (time division=0.1ms, voltage division=0.2 p.u.).

4 CONCLUSION

The energization overvoltages of Offshore Wind Farms (OWF) is investigated in this paper in both time and frequency domain. Since energization of OWF can result in resonance phenomena, detailed wind turbine transformer model is applied based on measurement and black box modelling. When feeding cable length is in the way that travelling wave frequency matches the dominant resonance frequency of transformer, resonance overvoltages on the LV terminal of transformer can be observed which their amplitude may be 24-26 pu in no load condition. The parasitic (stray) capacitances of full frequency converter in synchronous wind turbine or capacitor banks in asynchronous one can effectively decrease the amplitude of resonance overvoltages. But, the main control of resonance overvoltages can be done with surge arrester, specially the ones in LV terminal.

The energization of two rows of wind turbines is studied. The simulation results show that the energization of the first row is the most severe one and the amplitude of overvoltages on HV terminal of transformers will be decreased for the rows energized sequentially after the first row.

The simulation of OWF energization in various situation, considering the HF model of wind turbine transformer, assists on industrial design, appropriate component selection, reliability as well as maintenance cost and time savings. The next step is to observe how the resonance overvoltage distributes along the transformer winding.

5 ACKNOWLEDGMENTS

Authors greatly appreciate Norwegian Research Center for Offshore Wind Technology (NOWITECH) which is sources of funding. This paper is part of PhD project in Work Package 4.

6 REFERENCES

[1] EWEA annual wind statistics in 2010. url:http://www.ewea.org/fileadmin/ewea_documents/documents/statistics/EWEA_Annual_Statistics_2010.pdf.

[2] L. Liljestrand, A. Sannino , H. Breder, and S. Thorburn, “Transients in Collection Grids of Large Offshore Wind Parks,” Wiley Inter science, vol. 11 Issue 1, Pages 45 – 61, 2008.

[3] I. Arana, J. Holbøll, T. Sørensen, A. H. Nielsen, P. Sørensen, and O. Holmstrøm, “Comparison of Measured Transient Overvoltages in the Collection Grid of Nysted Offshore Wind Farm with EMT Simulations”, International Conference on Power Systems Transients (IPST), 2009.

[4] V. Akhmatov, B. C. Gellert, T. E. McDermott, W. Wiechowski, “Risk of Temporary Over-Voltage and High-Voltage Fault-Ride-Through of Large Wind Power Plant”, in Proc. of 9th Int. Workshop on Large-Scale Integration of Wind Power into Power Systems, 2010.

[5] P. Sørensen, A.D. Hansen, T.Sørensen, C.S. Nielsen, H.K. Nielsen, L. Christensen, M. Ulletved, “Switching transients in wind farm grids” European Wind Energy Conference and Exhibition. May 2007.

[6] B. Gustavsen, “Study of Transformer Resonant Overvoltages Caused by Cable-Transformer High Frequency Interaction,” IEEE TPD, Vol. 25, No. 2, pp. 770-779, 2010.

[7] X. Yang, C. Yue and H. Xie, “A PMSG based Wind Farm Modelling for Electromagnetic Transient Study”, In proc. of Association of the Electricity Supply Industry of East Asia and the Western Pacific (AESIEAP) CEO Conf., 2009.

[8] B. Gustavsen, “Wide band modelling of power transformers,” IEEE TPD, Vol. 19, No. 1, pp. 414–429, 2004.

[9] B. Gustavsen and A. Semlyen, “Rational approximation of frequency domain responses by vector fitting,” IEEE TPD, Vol. 14, No. 3, pp. 1052–1061, 1999.

[10] ABB surge arrester POLIM-R-2N datasheet,url: http://www.abb.com/search.aspx?q=POLIM-R-2N&abbcontext=products.

[11] ABB surge arrester POLIM-C-N datasheet,url: http://www.abb.com/product/db0003db004279/c125739900636470c1256e45005c7215.aspx

[12] J. A. Martinez, D. W. Durbak, "Parameter Determination for Modeling Systems Transients-part V:Surge Arresters", IEEE TPD, Vol. 20, No. 3, pp. 2073-2078, 2005.

[13] T. Ackermann, Wind Power in Power Systems, John Wiley & Sons, p. 54, 2005.

[14] A. H. Soloot, H. K. Høidalen, B. Gustavsen," Frequency Domain Investigation of Switching Transients in Offshore Wind Farms", accepted to be published in IEEE PowerTech, 2011.

[15] L. Kocewiak, J. Hjerrild, and C. L. Bak, "Harmonic analysis of offshore wind farms with full converter wind turbines," in Proc. 7th International Workshop on Large Scale Integration of Wind Power and on Transmission Networks for Offshore Wind Farms, 14-15 October 2009, pp. 539-544.

[16] Y. Yasuda, N. Uno, H. Kobayashi, and T. Funabashi," Surge Analysis on Wind Farm When Winter Lightning Strikes", IEEE TEC, Vol. 23, No. 1, pp. 257-262, 2008.

[17] Chong Han, D. E. Martin, M. R. Lezama, " Transient Over-Voltage (TOV) and Its Suppression For a Large Wind Farm Utility Interconnection", in Proc. of International Conference on sustainable power generation and supply, pp. 1-7, 2009.